Journal of the European Ceramic Society 18 (1998) 1351–1356

PII: S0955-2219(98)00064-8
0955-2219/98/$—see front matter

Hydroxyapatite Precipitation: A Case of Nucleation–Aggregation–Agglomeration–Growth Mechanism

R. Rodríguez-Clemente,[a]* A. López-Macipe,[a] J. Gómez-Morales,[a] J. Torrent-Burgués[b] and V.M. Castaño[c]

[a]Institut de Ciència de Materials de Barcelona, CSIC, Campus UAB, E-08193 Bellaterra, Spain
[b]Departmento d'Enginyeria Química, UPC, c/ Colom 1, E-08222 Terrassa, Spain
[c]Departmento Física Aplicada y Tecnología Avanzada, Instituto de Física, UNAM, Aptdo. Postal 1-1010, Querétaro 76001, Mexico

Abstract

The interpretation of the precipitation data of hydroxyapatite in MSMPR systems presents several problems due to the lack of consistency of the classical nucleation–growth–agglomeration mechanism in the analysis of the Crystal Size Distribution. In the proposed model, the mechanism of formation of particles starts with a nucleation episode, followed by the aggregation of supercritical nuclei ruled by surface energy excess, which counterbalance the repulsive forces between particles. The aggregates agglomerate, forming solid bridges, and the agglomerates continue to grow as distinct particles due to repulsive forces. © *1998 Elsevier Science Limited. All rights reserved*

1 Introduction

Hydroxyapatite (HA), $Ca_5OH(PO_4)_3$, is the principal inorganic constituent of human hard tissues such as bones and teeth. It crystallizes in the hexagonal system, and its equilibrium crystal morphology is a combination of prism and bipyramid. The habit most frequently observed is typically prismatic. The HA particles in the human body is also prismatic with crystal sizes varying from 130×30 nm in teeth enamel to 20×4 nm in dentine and bones.[1] The preparation of nanosized HA is, thus, an interesting target in technologies using restorative biomaterials with HA, to mimic the sizes present in the human body.

The important observation in bones and teeth is the low crystallinity of the HA particles, evaluated by XRD methods, with diffraction domains being smaller than the particles. This fact points to the existence of particles formed by aggregation of precursor crystals of a few nm in size. This low crystallinity is also observed in the early stages of the HA precipitation,[2] although some authors[3] indicate a progressive ordered agglomeration of the initial elementary particles to yield a structured particle which presents, consequently, higher crystallinity. Furedi[4] suggests that chain-like agglomerations of ACP (amorphous calcium phosphate) precursor particles act as a template for the crystallization of OCP (octacalcium phosphate) and direct the formation of fibbers-like crystals of this phase.

HA has been synthesized in batch and continuous precipitation systems.[5,6] There is an enormous amount of literature dealing with the crystallization pathways of HA at 37°C, resulting in a general consensus on the existence of precursors of the ACP type and OCP type precursors. However, at higher temperatures (>85°C) the direct precipitation of HA or a very rapid transformation of the precursors into HA is observed. The crystal sizes distribution obtained in the precipitation at high temperatures ranges from submicrometre to several micrometres. However, a microscopic analysis of the samples shows the polycrystalline character of the elemental particles, indicating a process of particles formation by aggregation rather than by crystal growth. In this paper we discuss a possible mechanism of HA particles formation based on the observation of particles precipitated by continuous and batch precipitations by the mixing of calcium and phosphate salts solutions, and from the decomplexing of homogeneous solutions containing Ca-citrate and Na and K phosphates. A model is proposed where the surface energy minimization acts as the driving force for the aggregation process. The formation of nanophases in the

*To whom correspondence should be addressed.

biological systems is mimicked by a coprecipitation process.

2 Experimental

2.1 Continuous precipitation of HA in a MSMPR (mixed solution mixed product removal) reactor

In MSMPR reactors the crystal size distribution (CSD) depends on the nucleation and growth kinetics as well as the residence time distribution within the crystallizer. Under steady-state conditions the population balance is given by:[7]

$$\frac{d[G(L)n(L)]}{dL} + \frac{n(L)}{\tau} = 0 \qquad (1)$$

where $n(L)$ is the differential population density of crystals of size L, which is the number of particles of size L to $L+dL$ in a unit volume, $G(L)$ is the linear rate of growth and τ is the mean residence time within the crystallizer. For size-independent growth rate, the semilogarithmic plot of population density versus size yields a straight line with the slope $-1/G\tau$ and the intercept n°, the nucleation population density, related to the nucleation rate $\beta^\circ = n^\circ G$. The nonlinearity in ln $n(L)$ versus L plots for MSMPR crystallizers may result from: (i) secondary nucleation in a small finite size range, (ii) size-dependent growth rate, (iii) growth rate dispersion, and (iv) particle agglomeration.[8]

We have performed several experiments of precipitation of stoichiometric HA in a 450 ml MSMPR reactor at 358 K, constant pH = 9 and residence time of 30 min, by mixing solutions of $CaCl_2$ and K_2HPO_4, the composition of which was maintained at the molar ratio Ca/P = 1·67. Table 1 shows the experimental conditions and the values calculated of the hypothetical instantaneous initial supersaturation, β_o, considering activities and perfect mixing of the reactants. The same table also shows the yield of the precipitation process, and the value of the residual supersaturation, β_R, once the steady state is reached.

In the cases of HA precipitation described in Table 1, the analysis of the CSD in the range of detection of the size analyser (Coulter LS instrument), i.e. from 0·1 to 1000 μm, using the population density data from the plots of ln$n(L)$ versus L, it was observed an initial rise from $L = 0{\cdot}1$ to around $L = 1$ μm, followed by a decrease with a positive deviation from linearity and some minor maxima. See Fig. 1.

In principle, the analysis of these plots, without including the initial rise, could indicate a mechanism of particles formation dominated mainly by nucleation, growth and aggregation in the micrometer size range, with discrete sizes of the aggregates. However, the absence of individual particles with $L > 1$ μm in length suggests little effect of the crystal growth. See Fig. 2.

The initial increase in the ln $n(L)$ versus L plot from $L = 0{\cdot}1$ to around $L = 1$ μm possibly reflects the aggregation in the nanometric/colloidal range, yielding the so-called primary particles (or primary aggregates). The peculiar shape of this plot suggests that the particles formed by nucleation (not observed by the Coulter analyser) tend to aggregate in an orderedly manner, preserving the prismatic habit and forming primary aggregates. These aggregates continue to agglomerate by forming interparticle bonds until they reach the micrometer size range. The linear portion of the plot is characteristic of a size-independent rate of growth. Departure from linearity at larger particles indicates aggregation. The typical size of primary agglomerates, at ~0·1 μm, agrees with the TEM observation, which suggests an ordered agglomeration, because the resulting particles have polyhedral shapes characteristic of the equilibrium form of HAP. Another argument in favor of this particular mechanism is the short induction time of a few seconds for the precipitation of HAP at 373 K, as recorded by the pH variation or precipitation yield measurements. A crystal with such high interfacial energy as HAP grows according to a $K_G (\beta-1)^n$ mechanism with very small values of K_G. Thus, the formation of the submicronic particles observed seems to obey an nucleation-ordered aggregation mechanism.

2.2 Batch precipitation of HA from homogeneous solutions

In another set of experiments, HA was precipitated from Ca/citrate/phosphate and Ca/EDTA/phosphate homogeneous solutions using

Table 1. Experimental conditions and calculated supersaturations for HAP precipitation in a MSMPR reactor at 85°C, pH = 9. Residence time (τ) = 30 min. $\beta_o = IAP_o/K_{SP}$, $\beta_R = IAP_R/K_{SP}$, yield (%) = 100 ($[Ca]_{T,o}-[Ca]_{T,R}$)/$[Ca]_{T,o}$

	Feeding solution				*Residual solution in the steady state*					
Run no.	$[Ca]_{T,o}$ *(mol/l)*	$[P]_{T,o}$ *(mol/l)*	IAP_o	β_o	$[Ca]_{T,R}$ *(mol/l)*	$[P]_{T,R}$ *(mol/l)*	*I*	IAP_R	β_R	*Yield (%)*
1	0·25	0·15	$1{\cdot}67\times10^{-32}$	$2{\cdot}28\times10^{28}$	$5{\cdot}13\times10^{-3}$	$3{\cdot}08\times10^{-3}$	0·516	$9{\cdot}10\times10^{-43}$	$1{\cdot}25\times10^{18}$	97·9
2	0·40	0·24	$1{\cdot}80\times10^{-32}$	$2{\cdot}46\times10^{28}$	$4{\cdot}46\times10^{-2}$	$2{\cdot}68\times10^{-2}$	0·828	$3{\cdot}32\times10^{-37}$	$3{\cdot}19\times10^{23}$	88·5
3	0·50	0·30	$1{\cdot}83\times10^{-32}$	$2{\cdot}50\times10^{28}$	$9{\cdot}39\times10^{-2}$	$5{\cdot}63\times10^{-2}$	01·374	$4{\cdot}44\times10^{-36}$	$6{\cdot}09\times10^{24}$	81·2

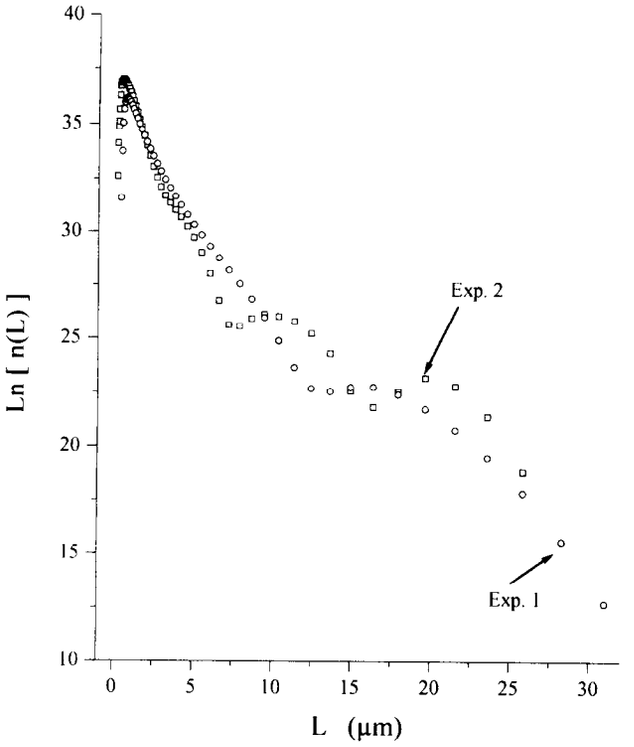

Fig. 1. Plot of the logarithm of the population density function $n(L)$ versus L for runs 1 and 2 of Table 1.

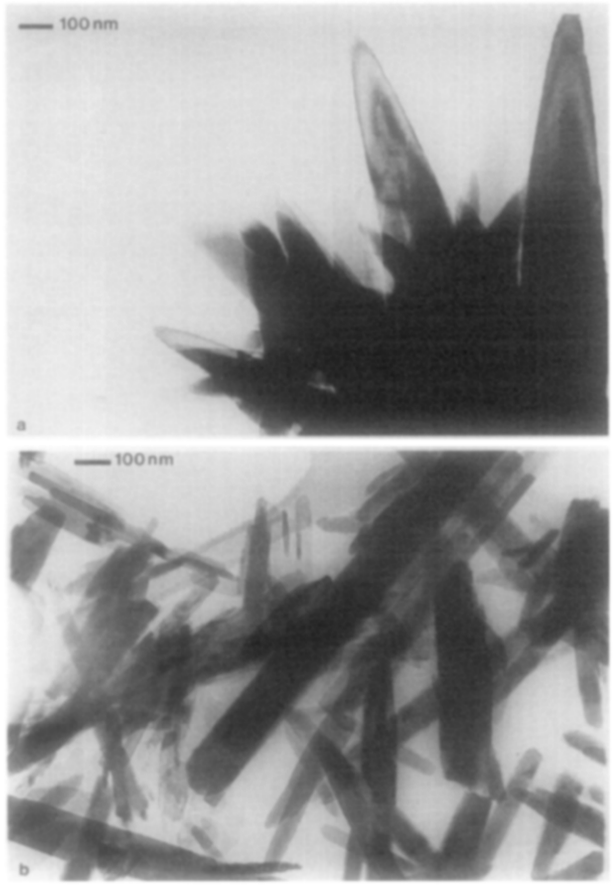

Fig. 2. Transmission electron micrographs of hydroxyapatite obtained in a MSMPR reactor. (a) Run 1; (b) Run 2.

microwave and conventional heating techniques under refluxing conditions. The Ca–citrate complexes were prepared from soluble $Na_3cit{\cdot}2H_2O$ or $K_3cit{\cdot}2H_2O$ salts. On heating these solutions the Ca–Cit complexes are decomposed resulting in solutions also supersaturated in Na_3cit, yielding a coprecipitate of this salt with HA particles in the nanometer size range of 30–60 nm. See Fig. 3.

However, in experiments using EDTA or $K_3cit{\cdot}2H_2O$ as Ca-complexing agents, larger HA particles of 300–500 nm appeared, similar to those obtained by continuous precipitation and no coprecipitation of the reactants salts was observed.

3 Discussion

Since the classical theory of Derjaguin–Landau–Verwey–Overbeek (DLVO), which considers a balance between repulsion forces due to the overlaps of the electric double layers of the particles and attractions in terms of London and van der Waals interactions,[9] several models of particle formation by nucleation and aggregation have been proposed in the literature, generally based on this theory[10,11] or an acid–base surface interactions[12] for non-directional aggregation, or in the influence of impurities and templates for directional aggregation.[13,14]

There are a number of interesting features related to the precipitation of HA in continuous and complexed-solutions batch reactors:

(a) The yield of solids decreases with the increase of the initial concentration, but is always higher than 80%.
(b) The residual thermodynamic supersaturation in the steady state of a continuous reactor is higher than 10^{18}, which is an enormous value in terms of the chemical potential of the solution.

The classical theory of nucleation relates the size of the critical nucleus to the supersaturation, interfacial energy of the system, and temperature through the well known relationship of the total free energy related to the formation of a nucleus of cubic shape and the characteristic size L:

$$\Delta G = 6L^2\gamma - L^3\Delta\mu/\Omega \qquad (2)$$

where γ is the interfacial energy, $\Delta\mu$ is the difference in the free energy between the solution and the crystal, $\Delta\mu = kT\ \ln(a/a_o) = kT\ \ln\beta_o$, expressed in joules, where a is the activity of the solute in solution, and a_o is the activity in equilibrium or the activity of the crystal, $\beta_o = \mathrm{IAP}/K_{SP}$, where IAP is the initial ionic activity product and K_{SP} is the thermodynamic activity product, and Ω is the volume of a molecule.

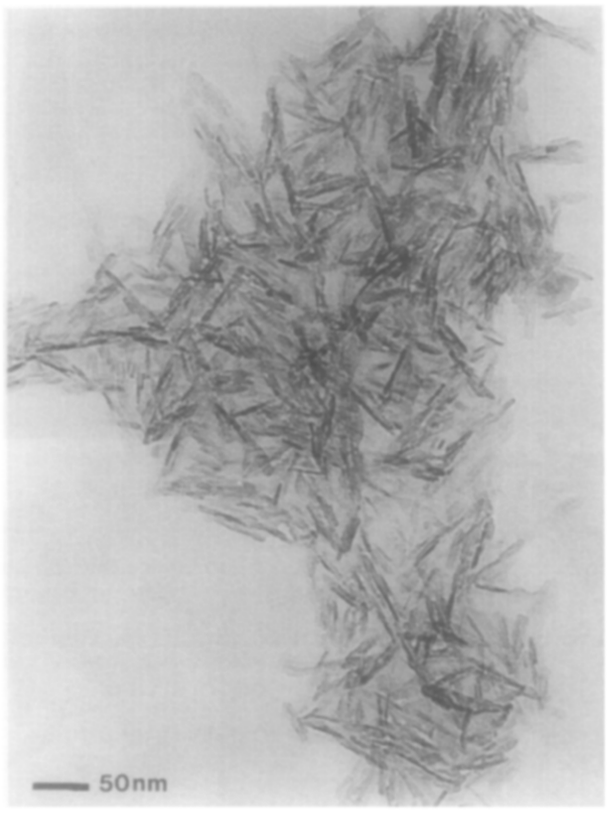

Fig. 3. Transmission electron micrographs of hydroxyapatite obtained by microwaves activated batch reactor using Ca–citrate complex solutions formed from $Na_3cit{\cdot}2H_2O$ reactants.

The size of the critical nucleus is related to the interfacial energy and the supersaturation by the relation:

$$L^* = 4\gamma\Omega/\Delta\mu = 4\gamma\Omega/kT\ln\beta_o \qquad (3)$$

For the case of hydroxyapatite, the interfacial energy[12,15,16] varies from an estimate of $\gamma = 160\,mJ/m^2$ to $9\,mJ/m^2$, $\Omega = 2{\cdot}64\times10^{-22}\,cm^3$ and $K_{SP} = [Ca]^5[OH][PO_4]^3 = 7{\cdot}3\times10^{-61}$ (at 85°C) where [] indicate activity. If we plot the two terms to the right of eqn (2), regarding the free energy balance associated with the formation of 1 mol of particles of size L, for various values of γ(HA) given in the literature (9–$160\,mJ/m^2$), a diagram showing the size of the critical nucleus which results at different values of the supersaturation β_o is obtained (Fig. 4). Taking a supersaturation of 10^{20} for $\gamma = 160\,mJ/m^2$ or a supersaturation of 2×10^{13} for $\gamma = 96$ yields a critical nucleus of $6{\cdot}4\times10^{-10}\,m$, which is the size of an HA molecule.

For a value of $\beta_o \approx 10^{10}$ the size of the critical nucleus varies from $1{\cdot}43\times10^{-9}\,m$ for $\gamma = 160\,mJ/m^2$ to much lower values with decreasing γ.

Considering residual supersaturation in continuous crystallization of $\beta_R > 10^{18}$, the nucleation of HA in this system appears to be non-classical. Essentially, there is no barrier for nucleation under the described experimental conditions, even at the steady state of the continuous precipitation process. This fact, together with the polycrystalline character of the particles, suggests that the mass precipitation process is essentially lead by nucleation; i.e. most of the solute crystallizes during the nucleation stage, while the crystal growth plays a minor role in the balance. The ordered aggregation of elementary nanocrystals, formed by nucleation, should therefore be responsible for the particle formation. Some crystal growth, at a constant residual supersaturation, may cause the cementing of the aggregates (agglomeration).

The energy balance, associated with the precipitation of 1 mol of supercritical nuclei at an initial instantaneous (ideal mixing of reactants) supersaturation β_o, results in:

$$\begin{aligned}\Delta G^*(\text{mol}) &= (V_M/L^{*3})6\gamma L^{*2} \\ &\quad - (V_M/L^{*3})\Delta\mu/\Omega L^{*3} \\ &= 6V_M\gamma/L^* - V_M\Delta\mu/\Omega \\ &= 6/4V_M\Delta\mu/\Omega - V_M\Delta\mu/\Omega \\ &= 1/2N\Delta\mu\end{aligned} \qquad (4)$$

where N is the Avogadro number.

The higher the initial supersaturation, the higher the gain of free energy released in the nucleation process due to the newly created surfaces. Considering that the system also holds an enormous free energy associated to the residual supersaturation, one should expect the relaxation of the free energy either by mass crystallization (crystal growth), or by a decrease in the total solid surface by an aggregation–agglomeration process, but NOT by nucleation (which will produce new excess surface free energy). An increase of 1 order of magnitude of the particles size, leads to a decrease of 1 order of magnitude of the excess surface energy G_S (Fig. 4). The larger the initial (or the residual) supersaturation, the higher the tendency for aggregation in order to release the excess free energy. This potential for aggregation is responsible for the absence of nanoparticles in a precipitation system.

The results observed in the precipitation from complexed Ca–citrate solutions also show peculiar mechanisms. The specific surface area measurements (BET method), XRD, FTIR and microscopy analyses show that in the case of precipitation from Ca/citrate/phosphate using sodium salts as reagents, the particle formation mechanism involves the initial precipitation of sodium citrate, which acts as a template. The heterogeneous nucleation of nanosized HA can also be interpreted in terms of surface free energy excess minimization by the interaction of the supercritical nuclei with this template. The lower value of the total surface free energy as compared to the continuous precipitation system avoids the need for the

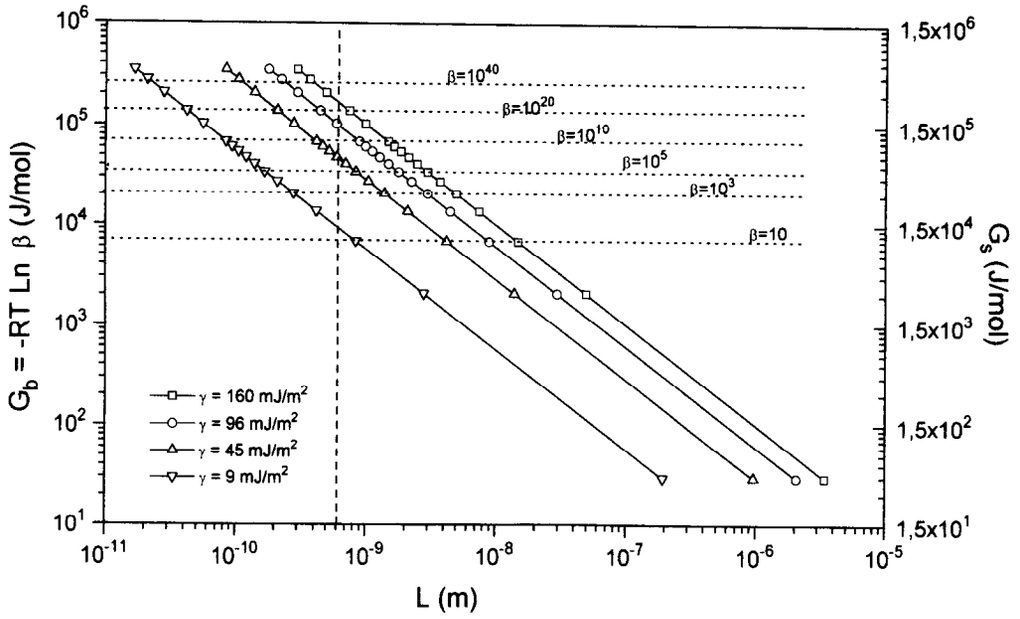

Fig. 4. Plot of the bulk (G_b) and surface (G_s) free energy balance associated with the nucleation of 1 mol of hydroxyapatite particles of size L and different interfacial energy, as reported in the literature.[12,15,16] The vertical line indicates the characteristic size of one hydroxyapatite molecule.

formation of primary aggregates. Afterwards, these nuclei grow to their final nanometer size, the template–particle interaction prevents the formation of HA aggregates and, thus, allows the formation of primary nanosized particles. The formation of HA nanoparticles in the presence of a templates, such as collagen was observed.[17]

It is interesting to note that the initial precipitation of a metastable phase which later dissolves, or the coprecipitation of both phases simultaneously, offers a unique way to obtain nanosized solid phases in natural and artificial crystallization from solution, which would otherwise be impossible to obtain due to surface energy excess.

4 Conclusions

- The precipitation of HA from solutions in a MSMPR and batch reactors is a nucleation–aggregation–agglomeration growth process.
- The aggregation process is ruled by surface energy minimization. This fact is reflected in the final crystal size distribution (CSD).
- A succesive precipitation process, where Na_3–cit·$2H_2O$ acts as template of the heterogeneous nucleation of HA, produces uniform nanosized HA particles.

Acknowledgements

This work has been supported and financed by the Project CICYT MAT95-1010-C03-01 of the Spanish National Plan of Research and CYTED VIII.6. The Spanish authors of this work belong to the Excellence Research Team GRQ93-8044, supported by the Autonomous Government of Catalonia. Critical reviewing editing of this manuscript by E. Matijevic is kindly acknowledged.

References

1. LeGeros, R.Z., *Monographs in oral science volume 15. Calcium phosphates in oral biology and medicine*, ed. H.M. Myers. Karger, New York, 1991, p. 1.
2. Eanes, E. D., Gillessen, I. H. and Posner, A. S., Intermediate states in the precipitation of hydroxyapatite. *Nature*, 1965, **23**, 365–367.
3. Lazic, S., Microcrystalline hydroxyapatite formation from alkaline solutions. *J. Cryst. Growth*, 1995, **147**, 147–154.
4. Füredi-Milhofer, J. H., Brecevic, L. J., Oljica, E., Purgaric, B., Grass, Z. and Perovic, G., *Particle Growth in Suspension*, ed. A.L. Smith. Academic Press, New York, 1973, pp. 109–120.
5. López-Macipe, A., Gómez-Morales, J. and Rodríguez-Clemente, R., Hydroxyapatite nanoparticles precipitation from homogeneous Ca–citrate complexed aqueous solutions using microwaves and conventional heating. *Adv. Mater.*, 1998, **10**, 19–53.
6. Gómez-Morales J., Torrent-Burgués J., Fraile-Sainz J. and Rodríguez-Clemente R., Precipitation of stoichiometric hydroxyapatite in a continuous flow MSMPR reactor. Submitted to Chem. Engng. Sci., 1997.
7. Randolph, A. D. and Larson M. A., *Theory of Particulate Processes*, 2nd edn. Academic Press, New York, 1986.
8. Midlarz, J., An exponential–hyperbolic crystal growth rate model. *Cryst. Res. Tecnol.*, 1995, **30**, 747–761.
9. Shaw, D. J., *Introduction to Colloids and Surface Chemistry*, 3rd edn. Butterworths, London, 1980.
10. Bogush, G. H. and Zukoski, C. F., Uniform silica particle precipitation: an aggregative growth model. *J. Coll. Int. Sci.*, 1991, **142**, 19–34.
11. Stavek, T. and Ulrich, J., A possible new approach to the better understanding of crystallization kinetics. *Cryst. Res. Technol.*, 1994, **29**, 465–484.

12. Liu, Y. and Nancollas, H., Crystallization and colloid stability of calcium phosphate phases. *J. Phys. Chem.*, 1997, **101**, 3464–3468.
13. Ocaña, M., Rodríguez-Clemente, R. and Serna, C. J., Uniform colloidal particles in solution: formation mechanism. *Adv. Mater.*, 1995, **7**, 212–216.
14. Furedi-Milhofer, H., Investigations of complex precipitation systems. *Croat. Chem. Acta*, 1980, **53**, 243–254.
15. Christoffersen, J. and Christoffersen, M.R., Kinetics of dissolution of calcium hydroxyapatite. *J. Cryst. Growth*, 1982, **57**, 21–26.
16. Boistelle, R. and López-Valero, I., Growth units and nucleation: The case of calcium phosphates. *J. Crystal Growth*, 1990, **102**, 609–617.
17. Wang, R. Z., Cui, F. Z., Lu, H. B., Wem, H. B., Ma, C. L. and Li, H. D., Synthesis of nanophase hydroxyapatite/collagen composite. *J. Mat. Sci. Letters*, 1995, **14**, 490–492.